Wind and Structures, Vol. 7, No. 2 (2004) 131-144
DOI: http://dx.doi.org/10.12989/was.2004.7.2.131

An active grid for the simulation of atmospheric boundary layers in a wind tunnel

A. Talamelli†

DIEM, Dipartimento di Meccanica e Aeronautica, Università di Bologna, Italy

L. Riparbelli‡

Dipartimento di Ingegneria Aerospaziale, Università di Pisa, Italy

J. Westin‡†

KTH Mechanics, Stockholm, Sweden

(Received March 2, 2003, Accepted December 1, 2003)

Abstract. A technique for the simulation of atmospheric boundary layers in wind tunnels is developed and tested experimentally. The device consists of a grid made of seven horizontal and vertical evenly distributed bars in which air injection holes are drilled in order to influence the flow in the wind tunnel. The air flow in each bar can be controlled independently. Firstly, the device is used together with a rough carpet, which covers the test section floor, in order to simulate the boundary-layer characteristics over an open rural area. Hot-wire measurements, performed at different positions in the test-section, show the capability of the grid in generating the required boundary layer. An acceptable agreement with statistical values of mean velocity and turbulence profiles has been achieved, together with a good span-wise homogeneity. The results are also compared with those of a passive simulation technique based on the use of spires.

Keywords: wind tunnel tests; atmospheric boundary layers simulation; active grid; turbulence profiles; hot-wire measurements.

1. Introduction

The use of wind tunnel experiments to study how structures and buildings interact with the wind in a region near the surface of the earth is still of fundamental importance. For this type of problems, numerical techniques, such as direct numerical simulations (DNS) and Reynolds Averaged Navier Stokes equations (RANS), are still limited, respectively, by the extremely high Reynolds numbers involved and by the lack of reliable turbulence models.

Two methods are normally used for the simulation of neutral atmospheric boundary layers in a

† Associate Professor
‡ Graduate Student
‡† Research Engineer

wind tunnel. The first is based on the natural growth of the boundary layer along a rough surface. The roughness elements should be of a size and density characteristic of the terrain surrounding the site and extend sufficiently far downstream for the required turbulent shear layer to become fully established. This may give a good representation of the real conditions, but very long test sections are required (Cermak 1982). However, most of the wind tunnels have smaller and shorter test sections than required, so it is necessary to accelerate the growth of the boundary layer thickness artificially. This can be done by introducing special devices at the entrance of the test section that modify the momentum distribution across the boundary layer, generating the same losses as can be achieved by a longer region of roughness elements.

These artificial devices can be divided in two main classes, passive and active. The main difference is that the latter provide an additional source of energy in the flow, e.g., air injection, pulsating grids or moving airfoils. Passive devices, instead, can be any kind of “static” obstacle (e.g., a barrier) positioned inside the mean flow.

Among passive devices, the most commonly used are barriers, spires and vortex generators. The barriers provide the initial momentum deficit near the ground level representing the effect of a longer boundary layer development. The simplest form of a barrier is a plane solid wall. However, barriers produce features which are inconsistent with a naturally grown boundary layer, i.e., separation bubbles or non-desired pressure gradients, which limit their maximum height. These effects can be reduced by perforating the barrier. Moreover, the fetch of the roughness has to be long enough to let these effects decay and the boundary layer recovers. The use of spire arrays in combination with floor roughness begun in the late 60’s and they are now widely employed in different shapes. The spires fulfil the dual role of a mixing device and barrier in a single component, and correctly distribute the momentum loss at the beginning of the test section. A simple shape of triangular flat spires was empirically developed by Irwin (1981).

The dimensions depend on the requested boundary layer shape and thickness. This method is focused on achieving the correct mean velocity profile; therefore turbulence intensity profiles and turbulence-generated scales must be checked “a posteriori” even though experimental results show that turbulence intensity and scales are not far away from full scale data. Elliptic wedge vortex generators (“shark fins”), followed by a barrier were firstly used by Counihan (1969). This shape has actually been designed to produce a distribution of turbulence that decay from a maximum value near the ground level to zero at the top of the generator. The boundary layer thickness is approximately equal to the height of the generator. The spacing between the generators, the height of the barrier and the relative distance between the barrier and the vortex generators are normally chosen by trial and error.

It must be pointed out that atmospheric boundary layers are highly variable in space and in time, and they are usually not known with a good accuracy. Therefore, in the design phase of a civil structure, a wind-tunnel simulation that brackets various probable conditions through families of velocity and turbulence profiles is certainly desirable. Different active techniques may be found in the literature. For instance, the tunnel itself may be directly driven by an array of blowers whose velocities can be independently controlled (Teunissen 1975). The Counter-jet technique (Nagib, *et al*. 1976) involves the use of upstream oriented wall jets with controllable injection velocities and angle to the ground. A round manifold tube is normally placed on the wind tunnel floor, at the entrance of the test section. Other techniques (see e.g., Schon and Mary 1971 and Sluman, *et al*. 1980) inject air through the wind tunnel floor in order to thicken the boundary layer. A porous plate may be placed at the beginning of the test section and the average injection velocity may be varied. Of course, which method is better depends on many parameters, like for instance the characteristics of the target boundary layer, the accuracy of the expected results, the cost and complexity of the equipment involved and finally the flexibility, i.e. the ability of simulating different conditions.

One important aspect that must be taken into account is the role of the roughness in the wind tunnel floor since it is strictly connected with the values of the law-of-the-wall parameters, related to the inner part of the atmospheric boundary layer. If the surface under consideration is lightly to moderately rough, like flat coastal or rural areas, then the simple use of a carpet or of gravel can be appropriate (Cook 1982). However, as the roughness increases, other elements of various size and geometry should be selected. There is not a universal method, and the selection of a suitable roughness has often been made by trial and error in order to reproduce the boundary layer parameters at appropriate scales (see Cermak 1982) even though some approximate procedure for selecting the appropriate roughness exist (see e.g., Gartshore and De Croose 1977).

In the present work a specific active simulation technique is studied. A specially designed grid, placed at the entrance of the test section, is used together with a rough carpet that covered the test section floor. Holes are made in the grid bars to inject air in the wind tunnel at a certain angle with respect to the mean flow in order to change both the momentum loss and the turbulence characteristics. The grid on the other hand generates a turbulent flow, providing a good mixing of the disturbances created by the injection. In order to investigate the effect on velocity profiles and turbulence characteristics, different parameters can be changed, i.e., wind tunnel speed, number of bars with air injection, flow rates through each bar and direction of injection.

The present work, funded by the Swedish Research Council for Engineering Sciences (TFR), is part of a study of the development and the interactions of the wakes behind wind turbines to explore the possibility to optimise the power output from wind farms by controlling the wake development behind upstream positioned wind turbines. In this context, as a first application of the grid, a boundary layer typical of an open rural area has to be simulated. In particular, the primary aim is to obtain a good representation of the logarithmic surface layer.

First, the effects on the flow and on the produced boundary layers due to different blowing conditions will be assessed. Comparison with the profiles obtained behind a passive grid and with those measured by means of spires will be shown. Required characteristics are realistic velocity, shear stress and turbulence profiles, a good spanwise homogeneity, and equilibrium conditions over the model test section. Results will also be compared with those reported in the comprehensive review by Counihan (1975) on adiabatic atmospheric boundary layers.

2. Experimental set-up and analysis procedure

All the experiments are carried out in the MTL-wind tunnel at the Department of Mechanics at KTH. The Minimum Turbulence Level (MTL) wind tunnel is a vertical closed return facility whose tunnel test section is only 7 m long, and can be considered relatively short for a correct simulation of atmospheric boundary layers. The cross-section dimensions are 1.2×0.8 m and the upper and lower walls are adjustable in order to be able to precisely control the streamwise pressure distribution. The wind tunnel is equipped with a heat exchanger positioned after the fan, in order to keep the air temperature constant and uniform within $\pm0.05^{o}$C.

The tunnel is driven by an 86 kW fan and the air speed can be controlled within 0-69 m/s. The circuit is ventilated to the surrounding atmosphere at the end of the test section where atmospheric pressure is provided. Before entering the test section, the flow passes through a honeycomb flow straightener and 5 screens, a settling chamber and the contraction, with a contraction ratio of 9 to

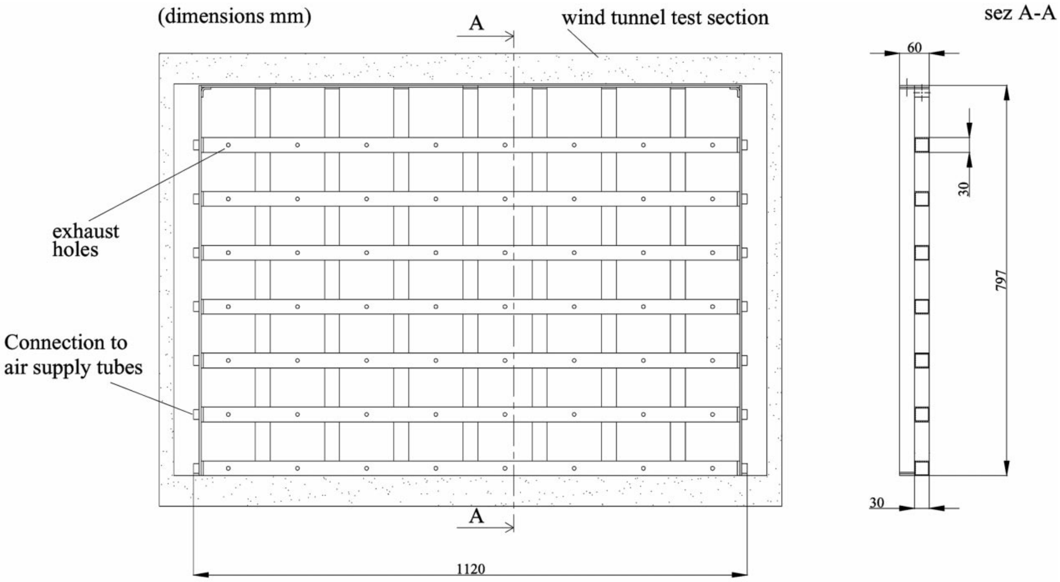

Fig. 1 Schematic view of the grid installed in the test section, without the air supply tubes

minimise the turbulence level. Characteristics and a description of the MTL wind tunnel are reported in Lindgren and Johansson (2002).

The grid (Fig. 1) is made by seven horizontal and vertical evenly distributed bars, and is characterised by a solidity ratio of 45%. Square bars are chosen in order to minimise the Reynolds number dependence of the pressure losses and turbulence intensity. In each horizontal bar, 8 air injection holes with a diameter of 8 mm are present. Air is supplied to the bars by a high-pressure fan connected to a stagnation chamber, and the pressure can be easily regulated by an exhaust valve. The air supply tubes are connected to both ends of each horizontal bar to obtain a symmetric flow distribution through the holes. Valves are connected to the tubes in order to control the airflow in each bar independently. Direction of injection, number of active bars and flow rates through each bar may be easily changed during the experiments. The lowest horizontal bar of the grid is positioned directly on the wind tunnel floor acting like a barrier. The test section floor is covered by a carpet characterised by protruding half-spherical elements, 3 mm high, distributed with regular intervals of 15 mm simulating the terrain roughness. A schematic of the experimental set-up is shown in Fig. 2.

In order to avoid a non-negligible increase of the mean velocity in a small region close to the roof of the test section, a small screen is mounted on top of the grid. The screen, with a fine mesh and low solidity (20%) increases the pressure drop near the upper wind tunnel wall, forcing the flow to decelerate. The mean velocity reaches a maximum (U_{max}) at a certain distance from the floor, and became smaller again approaching the top of the test section.

As far as the spires are concerned, they are designed following the empirical relation introduced by Irwin (1981). They consist of a tapered flat plate normal to the flow, and a splitter plate on the downwind side positioned at the entrance of the test section. The height of the spires, *h*, is evaluated from the power law index and boundary layer thickness requested, respectively α=0.16 and δ=0.5 m. The centrelines of the spires were separated with a spanwise interval of half the height of the spires. More information about the active grid and the spires can be found in Riparbelli (2000).

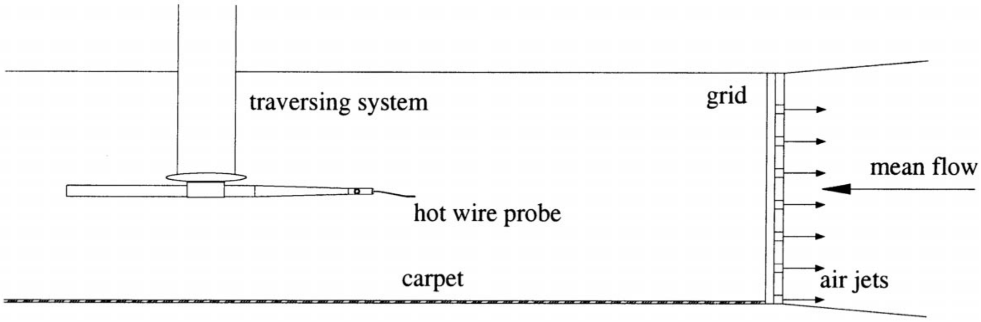

Fig. 2 Sketch of experimental set-up

Mean velocity and turbulence components are measured by means of constant temperature hot wire anemometry (CTA). A cross wire probe specially designed and built in order to measure close to the wall is used. A 5-axis computerised traversing system protruding from the roof of the wind tunnel allows a complete characterisation of the flow field. The output signals from the anemometers are conditioned and digitised by using a National Instruments A/D converter board (PCI-MIO 16-E4) with 12-bit resolution. The hot wires are calibrated in the free stream outside the boundary layer at different velocities and orientation to the mean flow. Two-dimensional fifth order polynomials are fitted by means of a least squared method to both the streamwise velocity (U) and to the ratio between wall-normal and streamwise velocity (V/U).

In the inner part of the boundary layer, the following logarithmic law can be used to fit mean velocity data

$$\frac{U}{U_*} = \frac{1}{k}\log\left(\frac{y-d}{z_0}\right) \tag{1}$$

where U is the mean velocity, y is the distance from the wall, k is a constant, generally assumed to be 0.4, U_* is the friction velocity, z_0 is the roughness parameter and d is a displacement height, usually very small or even zero for flat surfaces. Friction velocity is calculated from the Reynolds stress measurements, using the following relation:

$$\tau = \mu\frac{\partial U}{\partial y} - \rho uv \tag{2}$$

In the present evaluation, the contribution from the viscous term is neglected and the $\overline{uv}$ profile is extrapolated to $y=0$. The remaining unknowns, z_0 and d, were found as the parameters that minimised the error in the curve fit. Care must be taken in order to keep the right number of points that are included in the region where the law is valid (between 100 z_0 and 0.1 δ, see Nagib, *et al.* 1976).

Assuming that the mean velocity profile can be described by a simple power law,

$$\frac{U}{U_{ref}} = \left(\frac{y}{y_{ref}}\right)^{\alpha} \tag{3}$$

the value of the power law index α was found by a least-squares fit to the measured values. Thus, the displacement and momentum thickness δ^* and θ may be easily determined by integrating the experimental velocity profiles. Finally, the free stream velocity is identified by the maximum value reached in the profile, and the boundary layer height is found as the height where $U=0.99U_{\max}$.

Close to the carpet, although U is not linear in y, a straight line is used as an approximation from zero to the first measurement point. Integral length scales of the turbulence are evaluated by assuming that Taylor's hypothesis is valid following the relation described by Roach (1986).

$$L_u^x = \lim_{f \to 0}\left(\frac{U \cdot P(f)}{4u_{rms}^2}\right) \tag{4}$$

where f is the frequency and $P(f)$ is the power spectrum.

3. Results and discussion

3.1. Effect of blowing

In the following, results are reported for a measurement position fixed at 5.1 m, which is approximately where the models will be positioned for the real wind tunnel tests. In order to check the relative importance of blowing through different bars, the profiles measured behind the passive grid are compared with those obtained by activating an increasing number of bars, starting from the bottom. In Fig. 3 the mean profiles are scaled with the free stream velocity (U_e=6 m/s), while the turbulence intensity profiles are scaled with the local mean velocity (U). The wall-normal scale is normalised with the wind-tunnel height (H=0.8 m). Each bar carried the same amount of flow rate, the injection velocity (U_j) being fixed at 51 m/s. Firstly, it must be pointed out that the grid itself, even without any injection, considerably increases the boundary layer thickness as compared to a test section with only the carpet installed. This is mostly due to the bottom bar placed on the floor, which influences the flow downstream acting like a barrier. Fig. 3 shows that blowing has a clear effect on the velocity distribution. The boundary layer thickness is considerably increased; the passive grid generates a boundary layer thickness of 0.25 m (y/H=0.3), while the most effective active configuration, i.e., with three bars active, raises it up to 0.45 m (y/H=0.55).

If a power law is fitted through the data, a slight increase in the exponent a is observed, varying approximately from 0.19 to 0.21. However, the differences become less significant when the second and the third bar are added. From the above discussion it can be concluded that the boundary layer thickness can be augmented by injecting through the three bottom bars, the third being positioned at about 50% of the tunnel height. This is the order of magnitude of the boundary layer height generated downstream. Activating the upper bars does not add any advantage. On the contrary, it counteracts the effect of the lower bars, and when a uniform injection is set the boundary layer thickness is similar to the case with a passive grid.

The tests show that only the lower half of the grid may be used to increase the boundary layer thickness. The power index slightly changes with different blowing settings, while the roughness parameter z_0 shows negligible difference with a typical value of z_0=0.12 mm. It is possible that this parameter is mainly dependent on the characteristics of the carpet.

As far as the turbulence intensity is concerned, the figure shows that by activating the upper bars it is possible to modify the turbulence intensity in the central part of the boundary layer. The blowing does not seem to affect the intensity very close to the ground where a turbulence intensity of approximately 20% is achieved and in the top part of the boundary layer where freestream conditions are reached. The same behaviour is observed for the vertical turbulence intensity

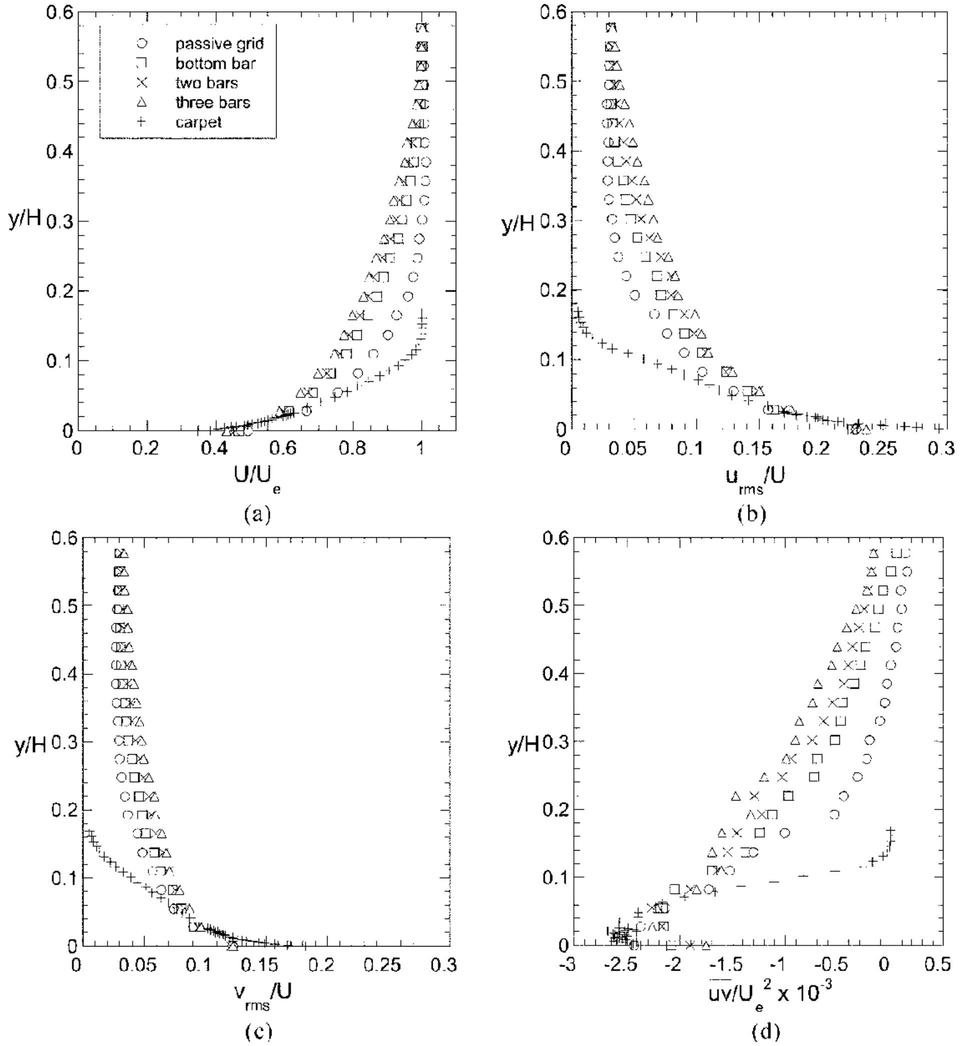

Fig. 3 Profiles obtained activating a different number of bars. Carpet: without grid. Free stream velocity U_e=6 m/s. Streamwise position x=5.1 m. Fixed injection velocity through each bar U_j=51 m/s. (a) mean axial component (b) turbulence intensity: axial component (c) turbulence intensity: wall-normal component (d) Reynolds stress.

component and for the shear stress profile.

However, if the same overall momentum is injected through a different number of bars (i.e., $\Sigma_j \rho A_j U_j^2$ is kept constant, where A_j is the hole area and U_j the velocity of the jets) the data almost collapse on each other, both for mean and turbulence components. In Fig. 4 mean velocity profiles are shown as an example. It may be concluded that as far as the boundary layer thickness and statistical values are concerned, the overall momentum injected seems to be a governing parameter independently whether the momentum is injected through the first one or the three bottom bars.

In Fig. 4 the effect of rotating the first bar, i.e. injecting the air vertically, is also reported. The mean velocity distribution follows the same trend as found before; moreover, no gain in spanwise

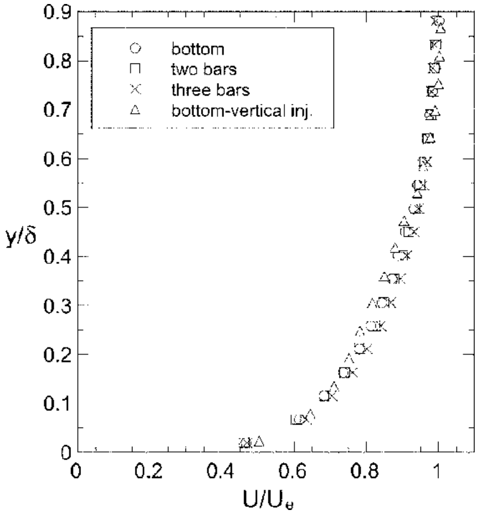

Fig. 4 Profiles obtained blowing through different bars with fixed overall momentum rate injected ($\Sigma_j \rho A_j U_j^2$). Free stream velocity U_e=6 m/s; x=5.1 m

homogeneity is achieved. These results seem to be in contradiction with some reported in the literature (see e.g., Nagib, *et al*. 1976). This may be partly explained by the strong difference in the injection velocities, which were much higher in the experiments by Nagib, *et al.* as compared to those adopted in the present one.

The effects of the injection depend considerably on the ratio between the injected momentum and the wind tunnel velocity. Fig. 5 shows the results obtained by measuring at a fixed position downstream x=5.1 m, keeping the wind tunnel velocity constant at 6 m/s and varying the injection rate. It can be seen that different injections result in different velocity distribution through the wind tunnel height. In Figs. 5a and 5b the data are scaled with the nominal free stream velocity and the wind tunnel height, in order to show the overall effect of injection. A first observation regards the boundary layer thickness, which increases with the increase of the injection velocity. By fitting a power law to these data, it is found that this is a family of profiles with index α varying from 0.19 to 0.21. As expected, mean components resemble those shown in Fig. 3, since the main governing parameter is the overall momentum injected.

The results in Fig. 5 are plotted together with those obtained with the use of spires. It is interesting that by means of the spires a considerable large boundary layer thickness can be obtained, i.e., approximately 90% of the height of the spires, corresponding to 80% of the tunnel dimension.

The shape and characteristics of the boundary layer profiles can be assessed in Figs. 5c and 5d where the wall normal distance is normalised with the boundary layer thickness. Note that the turbulence profiles in Fig. 5d are scaled with the local mean velocity (U). Significant are the differences both in the mean and in the turbulence profiles, even though the same turbulence intensities are obtained close to the wall.

In order to assess the quality of the obtained flow and to compare the two boundary layer generation techniques, measurements performed along the spanwise direction must be discussed. Fig. 6 shows the spanwise profiles of the mean streamwise and vertical components for both the active and the passive grid as well as the spires configuration, normalized with the spanwise average of

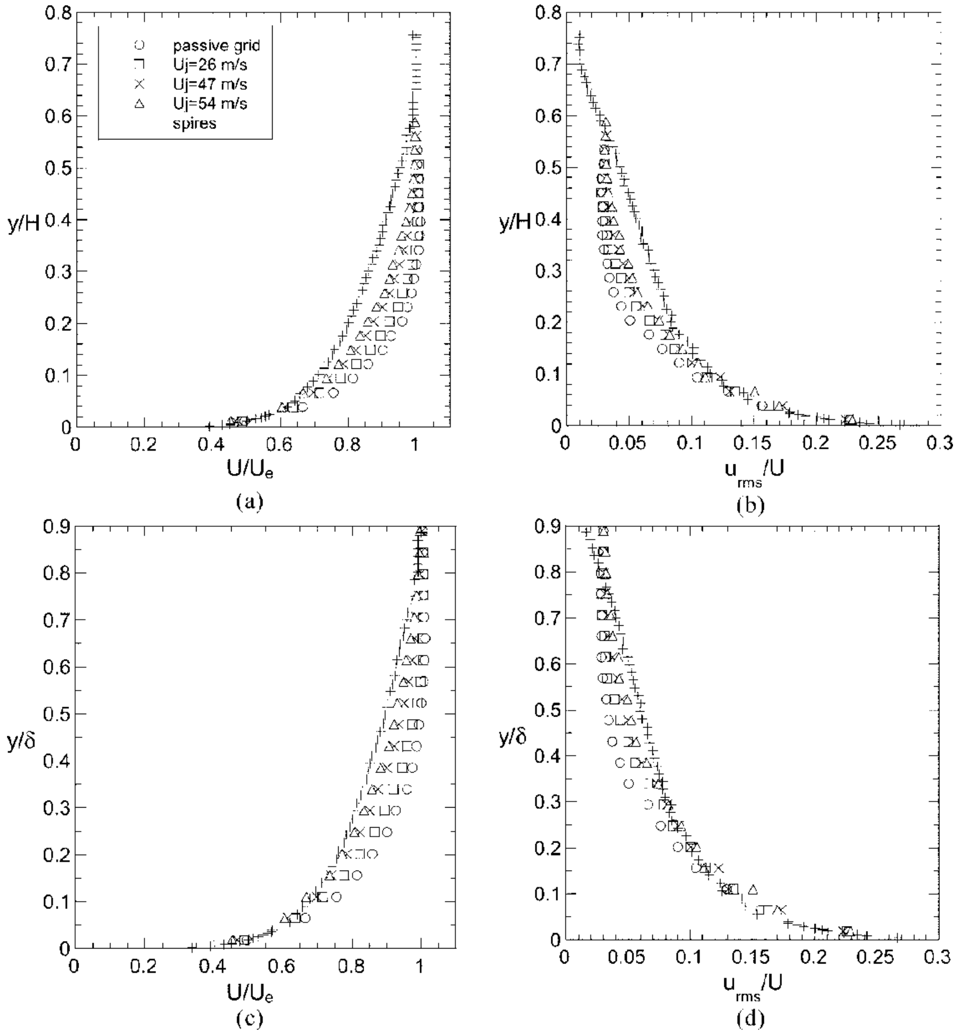

Fig. 5 Effect of varying the injected momentum rate and comparison with spires. Only the bottom bar is activated. Free stream velocity U_e=6 m/s, Streamwise position x=5.1 m. (a) mean velocity: streamwise component (b) turbulence intensity: streamwise component (c) - (d) same as (a) and (b) scaled with the boundary layer thickness.

the considered velocity component. It can be seen that behind the active grid a better spanwise homogeneity is obtained compared to the one measured behind the spires. Although the difference is small in U, it becomes much more evident for the V-component. The wave shape recalls the position of the spires, which introduce a discrete disturbance in the flow that persists downstream.

Considering the integral length scales of the turbulence produced by the active grid, it can be seen that by injecting through all the different bars the length scales do not change significantly. A slight increase can be observed when the air is injected, with approximately 10-15% increase in L_{ux} and 20-30% in L_{vx}. However, significant changes cannot be expected since the scales are related to the geometry and dimensions of the grid (Fransson 2001).

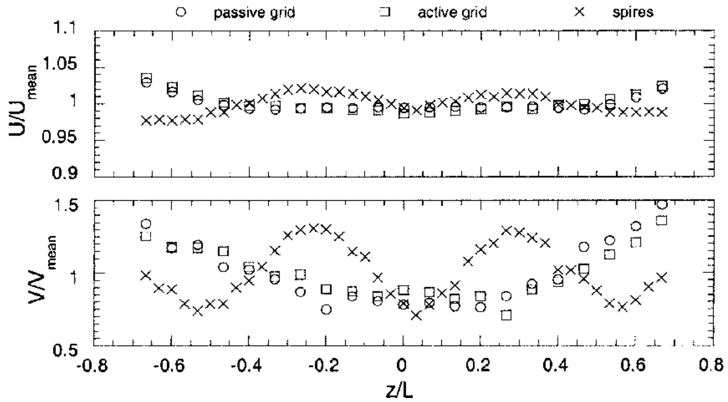

Fig. 6 Spanwise homogeneity at one streamwise positions x=5.1 m. Height above the ground y=320 mm (y/H =0.4). Free stream velocity U_e=10 m/s. U_j=50 m/s through the bottom bar

3.2. Application for the generation of an open rural area boundary layer

As a first application, the grid has been used to simulate a boundary layer typical of an open, rough or moderately rough, rural area.

Fig. 7 shows results obtained with the active grid using an injection velocity (U_j) of 51 m/s through the three bottom bars. The velocity profiles measured at three streamwise distances behind the grid almost collapse on each other, showing that the boundary layer develops downstream and assumes near-equilibrium state early in the test section (at about 50% of the test section length). In particular, the boundary layer maintains similar characteristics in mean velocity, while the shape of the turbulence profile is slightly modified downstream. The near-equilibrium characteristics are confirmed by the downstream evolution of the friction velocity and shape factor. This behaviour is probably related to the presence of the grid, which is believed to speed up the process of reaching a near equilibrium state.

Table 1 summarises the fitting parameters obtained at the test measurement position (x=5.1 m) for two different wind tunnel speeds. Values suggested by Counihan (1975) for similar terrain characteristics are also reported.

Before a comparison can be made between wind tunnel results and data from field measurements, a scale factor must be determined. Statistical turbulence measurements are reported for a particular height from the ground, which must be transformed to a specific wall-normal distance in the wind tunnel.

Since the boundary layer height is a poorly defined quantity being difficult to measure and since we are interested in the wind-tunnel simulation of the inner part of the boundary layer, the scaling may involve the roughness parameter z_0 and the height of the logarithmic region $\delta_{\log}$, i.e., the limit where the profile can be considered logarithmic. By comparing the values obtained in our experiments and those reported by Counihan it can be seen that z_0 does not help in finding a unique scale factor. Indeed, the range of z_0 values presented by Counihan for this type of terrain brings to the conclusion that any scale factor from 80 to 1600 is a plausible value. A more unique indication is given by the ratio between the $\delta_{\log}$ distances. In this case, a scale factor of about 1100, which lies in the range above, is obtained.

Considering the table it can be seen that the power index results are slightly higher in the wind

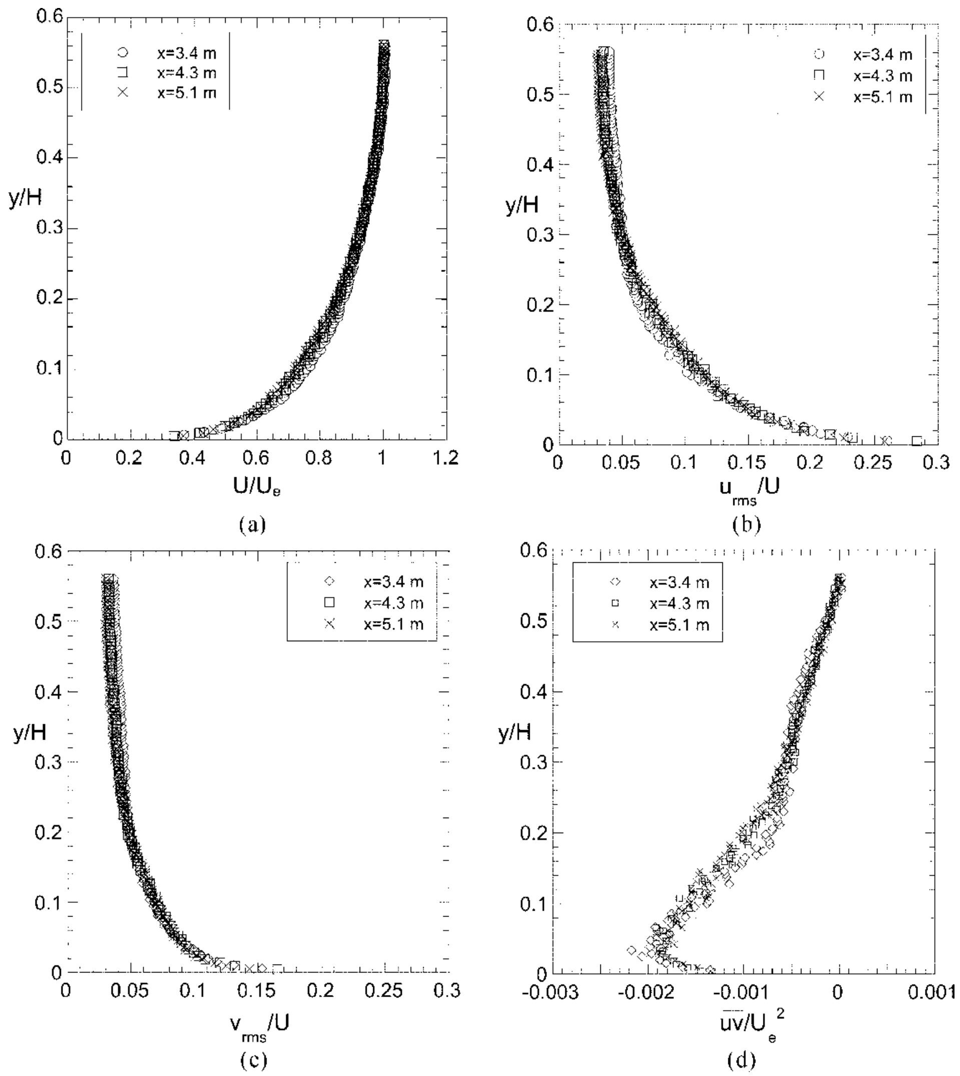

Fig. 7 Profiles of the mean and fluctuating axial component at different streamwise distances from the grid. Free stream velocity U_e=6 m/s. Fixed injection velocity through each of the three bar, U_j=51 m/s (a) mean axial component (b) turbulence intensity: axial component (c) turbulence intensity: wall-normal component (d) Reynolds stress

tunnel measurements as compared to those relevant for flat rural areas, and the present results are closer to a moderately rough surface. Besides, the turbulence intensity seems to be slightly higher than the proposed value. The reference position in the wind tunnel measurements, equivalent to 30 meters in the real ABL, has been estimated by using 1100 as a scale factor and corresponds to y/H~0.035.

The measured Reynolds stresses close to the ground level are between 0.002 and 0.0025, values larger than to the ones predicted by Counihan for this type of surface. However, in comparison to the other quantities considered, the available data for this type of measurement is subjected to a considerable scatter (cf. Couhinan).

Table 1 Characteristic values determined from the wind tunnel experiments and compared with typical values for a rural atmospheric boundary layer, as suggested by Counihan (1975)

	Active grid	Active grid	Counihan	Counihan/ Active grid
Position downstream the grid, **x** (m)	5.1	5.1		
Free stream velocity, $\mathbf{U_e}$ (m/s)	5.8	10.3		
Friction velocity, $\mathbf{U_*}$ (m/s)	0.262	0.482		
Boundary layer height, $\boldsymbol{\delta}$	~ 380 mm	~ 300 mm	~ 600 m	
Displacement thickness, **d** (mm)	2	3		
Roughness parameter, $\mathbf{z_0}$	0.125 mm	0.122 mm	0.01-0.15 m	80-1600
Logarithmic height, $\boldsymbol{\delta}$**log**	90 mm	90 mm	100 m	1100
Power Index $\boldsymbol{\alpha}$	0.21	0.19	~ 0.16	
$(u_{rms}/U)_{30\text{ m}}$	16-18%	16-18%	15%	
uv/U^2_{ref}	~ 0.002	~ 0.002	0.001-0.0015	
Lux (m)	0.13-0.15		120	800-900

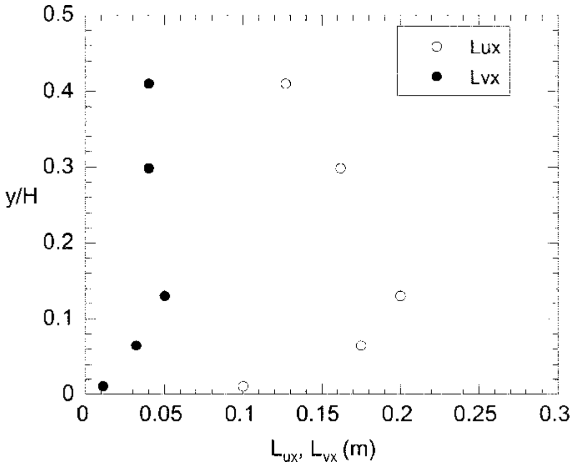

Fig. 8 Integral length scales measured at different wall-normal positions. Free stream velocity U_e=6 m/s. Streamwise position x=5.1 m

In Fig. 8 the available data on the length scales are presented. Both streamwise and wall-normal length scales *Lux* and *Lvx* increase with the height up to half of the boundary layer thickness. Thereafter they slightly decrease for an increase of height. This behaviour is consistent with the one observed in real *ABL*. At the reference position y/H=0.035, by interpolating the data in Fig. 8, an estimated value between 0.13 and 0.15 m is obtained. This value is close to the desired one. Indeed, for this type of terrain, a value of 120 m in the real *ABL* (see Fig. 12 in Counihan) gives a scale factor, which lies in between 800-900. As far as the *Lvx* is concerned the value obtained in the wind tunnel is too small. A typical ratio *Lux*/*Lvx* for atmospheric boundary layers is of the order of 1.3.

Fig. 9 presents an example of the power spectra measured inside the boundary layer. It is evident the decrease of the energy at low frequencies for the vertical component if compared with the longitudinal one, which is the responsible for the low value of *Lvx*.

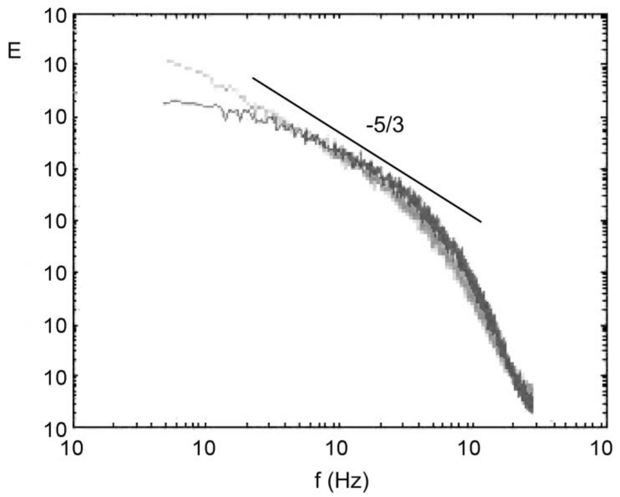

Fig. 9 Spectra evaluated in the boundary layer when the bottom bar is active. Free stream velocity U_e=6 m/s; boundary layer height 350 mm; y=52 mm

In conclusion, Table 1 shows that, with the present grid, a good indication on a possible scaling is obtained, even though some uncertainty, due to the high scatter in the real *ABL* statistical data, are present. Finally, it must be concluded that with the proposed method it is possible to simulate the inner part of the atmospheric boundary layer for the requested type of terrain. However, the scaling factor obtained is relatively high, which means that only small models can be placed in the wind tunnel. This fact may preclude the possibility to obtain well-detailed and accurate measurements around the model.

4. Conclusions

An active grid is designed and developed to explore the possibility of generating an atmospheric boundary layer in a wind tunnel with relatively short test section. A family of shear layers, which are typical of rural moderately rough terrain, with an indicative value of the power law index of 0.19-0.21, may be generated. Basically, the boundary layer thickness can be increased by injection through the bottom bars and it seems that the governing parameter is the total momentum injected disregarding if it is injected through the first one only or if it is distributed over all three bottom bars. Tests were carried out mostly with counter-flow (horizontal) injection. Upward injection (vertical) does not give any evidence of improved flexibility. An improved spanwise homogeneity of the flow is obtained if compared with spires. It is also proved that injection through all the bars slightly increases the turbulence levels throughout the boundary layer height, without changing the shape of the profile. Therefore, the obtained effects can be combined to give the possibility of controlling the boundary layer thickness and the mean velocity profile, by injection through the bottom bar, and changing turbulence levels by a uniform injection through the others. The influence of the active grid was proved to be stronger for lower velocities, and tests were carried out with an injected momentum of 14% of the mean flow. Stronger effects may be obtained by using two fans in parallel or a more powerful one.

The expected flexibility was less satisfactory regarding the influence on the power law α

describing the mean velocity profiles. In fact, although the injection velocity was varied from 0 to 54 m/s, α changed within a small range. On the other hand this shows that the floor roughness is still the most important factor defining the boundary layer characteristics. Once this is established, through a combined action with a controlled injection it is possible to adapt smaller changes through a regulation from outside, in order to bracket a broad range of wind conditions. If completely different situations have to be simulated, the grid remains installed while the roughness elements are changed.

The configuration presented here is a basic one, where many parameters can be changed and studied, in order both to characterise this device better and to improve it. For instance by changing the ratio between holes and rod diameter, by using variable spacing between each rod, higher pressure fan to increase jet velocities and by injecting with variable flow rates across the test section height.

Acnowledgements

The authors wish to thank Mr. Ulf Landen and Mr. Marcus Gallstedt for their help with the manufacturing of the experimental set-up. We are in debt with Prof. Henrik Alfredsson and Prof. Gianni Bartoli for their fruitful suggestions. Swedish TFR and Italian CNR are also acknowledged.

References

Cermak, J.E. (1982), “Physical modelling of the atmospheric boundary layer (ABL) in long boundary layer wind tunnels (BLWT)”, *Proceedings of the International Workshop on Wind Tunnel Modelling Criteria and Techniques in Civil Engineering Applications*, Gaithersburg, Maryland, USA, Cambridge university press.

Cook, N.J. (1982), “Simulation techniques for short test-section wind tunnels: roughness, barrier and mixing-device methods”, *Proceedings of the International Workshop on Wind Tunnel Modelling Criteria and Techniques in Civil Engineering Applications*, Gaithersburg, Maryland, USA, Cambridge university press.

Counihan, J. (1969), “An improved method of simulating an atmospheric boundary layer in a wind tunnel”, *Atm. Environment*, **3**, 197-214.

Counihan, J. (1975), “Adiabatic atmospheric boundary layers: a review and analysis of data from the period 1880-1972”, *Atm. Environment*, **9**, 871-905.

Fransson, J. (2001), “Investigations of the asymptotic suction boundary layer”, TRITA-MEK Licentiate Thesis 2001:11, KTH Mechanics, KTH, Stockholm, Sweden.

Gartshore, I.S. and De Croose, K.A. (1977), “Roughness element geometry required for wind tunnel simulations of the atmospheric wind”, *ASME paper* no. 76-WA/FE-18.

Irwin, H.P.A.H. (1981), “The design of spires for wind simulation”, *J. Wind Eng. Ind. Aerodyn.*, **7**, 361-366.

Lindgren, B. and Johansson, A.V. (2002), “Evaluation of the flow quality in the MTL wind-tunnel”, TRITA-MEK Technical Report 2002:13, KTH Mechanics, KTH, Stockholm, Sweden.

Nagib, H.M., Morkovin, M.V., Jung, J.T. and Tan-atichat, J. (1976), “On modelling of atmospheric surface layers by the counter-jet technique”, *AIAA Journal*, **14**(2), 185.

Riparbelli, L. (2000), “Wind tunnel simulation of Atmospheric Boundary Layers by means of an active grid”, M. Sc. Thesis, Department of Aerospace Engineering, Università di Pisa.

Roach, P.E. (1986), “The generation of nearly isotropic turbulence by means of grids”, *Technical Report*, Advanced Research Laboratory Rolls Royce plc.

Schon, J.P. and Mary, P. (1971), “A preliminary study of the simulation of neutral atmospheric boundary layer using air injection in a wind tunnel”, *Atmospheric Environment*, **5**, 299-311.

Sluman, T.J., Van Maanen, H.R.E. and Ooms, G. (1980), “Atmospheric boundary layer simulation in a wind tunnel, using air injection”, *Applied Scientific Research*, **36**, 289-307.

Teunissen, H.W. (1975), “Simulation of the planetary boundary layer in a multiple-jet wind tunnel”, *Atm. Environment*, **9**, 145-174.

GS